J Neurophysiol 91: 1050–1063, 2004.
First published October 15, 2003; 10.1152/jn.00652.2003.

The Role of Execution Noise in Movement Variability

Robert J. van Beers,[1,2,3] Patrick Haggard,[1] and Daniel M. Wolpert[2]

[1]*Institute of Cognitive Neuroscience, University College London, London WC1N 3AR;* [2]*Sobell Department of Motor Neuroscience, Institute of Neurology, University College London, London WC1N 3BG, United Kingdom; and* [3]*Department of Neuroscience, Erasmus MC, 3000 DR Rotterdam, The Netherlands*

Submitted 8 July 2003; accepted in final form 10 October 2003

van Beers, Robert J., Patrick Haggard, and Daniel M. Wolpert. The role of execution noise in movement variability. *J Neurophysiol* 91: 1050–1063, 2004. First published October 15, 2003; 10.1152/jn.00652.2003. The origin of variability in goal-directed movements is not well understood. Variability can originate from several neural processes such as target localization, movement planning, and movement execution. Here we examine variability resulting from noise in movement execution. In several experiments, subjects moved their unseen hand to visual targets, under conditions which were designed to minimize the variability expected from localization and planning processes. We tested short movements in 32 directions in a center-out reaching task. The variability in the movement endpoints and in the initial movement direction varied systematically with the movement direction, with some directions having up to twice the variability of others. In a second experiment we tested four movements in the same direction but with different extents. Here, the longer movements were systematically curved, and the endpoint ellipses were not aligned with the straight line between starting and end position, but they were roughly aligned with the last part of the trajectory. We show that the variability observed in these experiments cannot be explained by planning noise but is well explained by noise in movement execution. A combination of both signal-dependent and signal-independent noise in the amplitude of the motor commands and temporal noise in their duration can explain the observed variability. Our results suggest that, in general, execution noise accounts for at least a large proportion of movement variability.

INTRODUCTION

A ubiquitous feature of human motor control is the variability of our movements that limits the accuracy with which we can perform a task. Indeed society places a premium on consistent accuracy to the extent that those who can reliably hit a ball with a club into a hole are often financially well rewarded. However, even these skilled sportsmen and women show some variability in movement. The origin of this variability within the sensorimotor system is not well understood, but it may arise from processes being corrupted by noise. The precise characteristics of the variability could indicate where the noise arises.

Here we focus on goal-directed arm movements. Producing an arm movement can be thought to consist of three stages: localization, planning, and execution. In the localization stage, the locations of the target and the hand are derived from sensory information. Movement planning refers to the selection of motor commands that can produce the movement from the initial to the target position. It uses the outputs of the localization stage, namely target and hand position, as input and generates motor commands as the output. In the movement execution stage, the planned motor commands are sent to the muscles so that the movement is actually made. This process can be under feedback control (Miall and Wolpert 1996).

The neural signals at all these stages will be noisy. The observed movement variability will therefore reflect the noise at each of the three stages, but it is possible that different stages contribute to very different degrees and that these contributions will depend on the experimental conditions. For instance, when the target position is made highly uncertain because it has to be memorized in the dark (McIntyre et al. 1998), the uncertainty in target localization can be so large that this is the major source of variability. Its contribution will however be relatively minor when the target remains visible (Hansen and Skavenski 1977), especially when it is seen in a structured visual field (Conti and Beaubaton 1980). The contribution of hand localization will also be small when the hand is seen at movement onset (van Beers et al. 1996), especially when the target and hand are seen simultaneously (Rossetti et al. 1994), but can be appreciable when the hand cannot be seen (Desmurget et al. 1995; van Beers et al. 1998).

Several studies attributed movement variability to the movement planning process. For instance, Gordon et al. (1994b) observed that endpoint ellipses (confidence ellipses on the spatial distribution of movement endpoints) align with movement direction and that ellipse shape varies with movement extent. Their interpretation was that movements are planned as a vector from the initial hand position to the target position and that the direction and extent of this vector are planned independently, each having their own, independent noise. The idea that planning noise is the major source of movement variability has been very influential (e.g., McIntyre et al. 1997; van den Dobbelsteen et al. 2001; Vindras and Viviani 1998). However, these studies fail to provide evidence that all the observed variability arises in the planning process and not at other stages.

Movement execution will inevitably give rise to movement variability because motor output (motor commands, muscle contractions, or muscle torques) is inherently variable. This is evident in the noise in the force produced during isometric muscle contraction (Jones et al. 2002; Schmidt et al. 1979; Slifkin and Newell 1999). Several authors (Harris and Wolpert 1998; Meyer et al. 1988; Schmidt et al. 1979; van Galen and de Jong 1995) have proposed that noise arising in the motor output stage gives rise to substantial movement variability, which could explain the speed-accuracy trade-off known as Fitts' law (Fitts 1954). However, the assumption that motor

Address for reprint requests and other correspondence: R. J. van Beers, Dept. of Neuroscience, Erasmus MC, P.O. Box 1738, 3000 DR Rotterdam, The Netherlands (E-mail: r.vanbeers@erasmusmc.nl).

The costs of publication of this article were defrayed in part by the payment of page charges. The article must therefore be hereby marked "*advertisement*" in accordance with 18 U.S.C. Section 1734 solely to indicate this fact.

execution processes produce considerable movement variability has never been verified. The aim of this study was to determine the magnitude of movement variability that is caused by noise in movement execution and therefore to assess the importance of this noise.

Our approach is to analyze the variability of pointing movements made in conditions in which the effects of localization and planning noise are minimized. To investigate whether the observed noise is caused by execution noise, we tested movements in different directions and of different extents. The underlying idea is that movements with different spatial paths require very different motor commands due to the kinematics and dynamics of the arm (Koshland et al. 1999). Therefore movement variability that is caused by execution noise will vary in a systematic and predictable way with movement direction. In contrast, variability caused by localization and planning noise will, if expressed as a component in the movement direction and a component in movement extent, not vary with direction or will do so in a way that is independent of the arm's kinematics and dynamics and will therefore be quite different from the variability due to execution noise.

METHODS

Subjects

After providing informed consent, 15 subjects (11 female, 4 male), 18–34 yr old, participated in this study. A local ethics committee approved the experimental protocols. None of the subjects reported any sensory or motor deficits, and all had normal or corrected-to-normal vision. Ten subjects participated in *experiment 1*, seven were tested in *experiment 2* (6 of which participated also in *experiment 1*), and four new subjects participated in *experiment 3*. All but one subject reported being right-handed. The left-handed subject participated only in *experiment 1*; her results were not systematically different from those of the right-handed subjects.

Apparatus

Subjects pointed with the tip of their right index finger to visual targets on a horizontal table slightly below shoulder level. They sat on a chair with their head resting on a chin rest (see Fig. 1*A*). The setting allowed only little movement of the trunk; therefore the shoulder position was approximately fixed. Two splints immobilized the wrist and index finger so that arm movements could only be made by shoulder and elbow rotation. The subjects looked down in a horizontal mirror placed midway between the tabletop and a rear-projection screen on which visual objects could be projected. This allowed (virtual) vision of the table and visual objects while the arm could not be seen. The room was illuminated to produce a structured visual field in which localization of visual targets is optimal (Conti and Beaubaton 1980).

In *experiments 1* and *2*, a receiver of a Fastrak motion tracker (Polhemus, Colchester, VT) was attached to the subject's fingertip to record its position at 120 Hz (accuracy: better than 1 mm). The visual objects were displayed by a Pioneer RVD-XG10ED LCD projector (Pioneer, Tokyo, Japan). The projector displayed images generated by a PC at 90 Hz with a resolution of 1024 × 768 pixels on an area of about 68 × 84 cm on the projection screen. Three different objects could be shown: the starting position (a 4.5-mm-radius green disc), the target (a 5.5-mm-radius yellow disc), and a cursor at the current finger position (a 3.5-mm-radius red disc). The background was black. The output from the projector and the Fastrak was calibrated before each session using a 6 × 4 grid of positions covering the whole workspace. The calibration procedure was based on two-dimensional quadratic regressions, which were used on-line during the experiment for displaying the objects.

In *experiment 3* we used a similar setup, apart from the following differences. The subject's right arm was supported by an air-jet system so that the arm could move frictionless over the table, and the fingertip never touched the tabletop. The trunk was strapped to the chair to prevent translational movement of the shoulder. Finally, movements were recorded with an Optotrak 3020 system (Northern Digital, Waterloo, Ontario, Canada; accuracy: 0.5 mm).

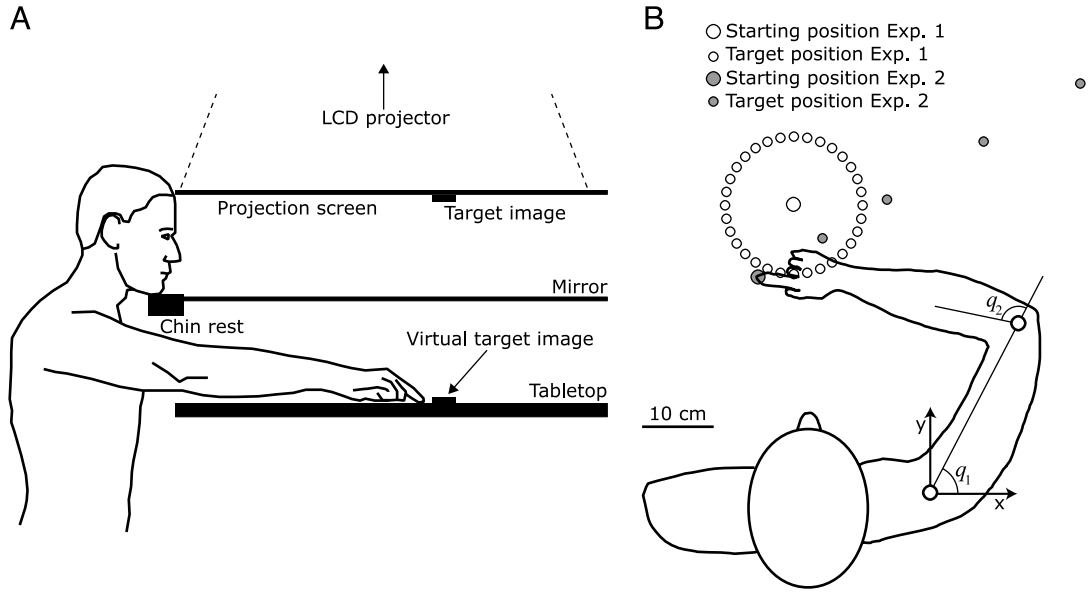

FIG. 1. Experimental setup. *A*: side view. Subjects moved their hand to targets on the tabletop. The mirror occluded the subject's arm from vision and made visual objects displayed on the projection screen by an LCD projector appear as if they were located on the tabletop. In this way, the subject could see visual targets, and at certain phases within the experiment, a cursor at the fingertip position, whereas the arm could never be seen. *B*: top view with starting and target positions used in *experiments 1* and *2* and definition of joint angles q_1 and q_2 and x and y directions.

Procedure

Subjects pointed at visual targets without visual feedback about their movements. Each trial started with a presentation of the starting position. The finger position cursor was shown simultaneously to help the subject to bring the finger quickly and accurately to this location. The target appeared when the finger had been kept for 500 ms within 5 mm from the center of the starting position. The task was to make a quick, uncorrected movement toward the target. No other instructions about the speed were given, so that subjects made fairly quick, natural movements. In *experiments 1* and *2*, subjects touched the table on the starting position, they lifted their hand at movement onset, and touched the table again at the end of the movement. The elbow or other parts or the arm never touched the table. In *experiment 3*, no part of the hand or arm ever touched the table. In all experiments, the finger and starting position discs were extinguished when the speed first exceeded 5 cm/s (at that time, the finger usually had moved approximately 1 mm). The target circle was extinguished when the speed first fell below 5 cm/s while the finger was closer to the target than to the starting position. At this moment, the starting position appeared again, after which subjects moved their finger back to that location. The finger position cursor was shown from the moment the fingertip was closer to the starting than to the target position. In this way, subjects never had any feedback about their movement endpoints or about the finger position during the reaching movement. All data were saved for off-line analysis.

EXPERIMENT 1. Movements from a central starting position, 20 cm to the left and 43 cm in front of the right shoulder, toward 32 equally spaced targets were tested (see Fig. 1*B*). Target distance was 9.6 cm. We used a blocked design in which a block consisted of 30 movements to a single target. The order of blocks was random, and successive blocks were separated by 1-min breaks. We chose a blocked design to minimize the variability caused during movement planning. It allowed subjects to refine their choice of motor commands for each target so that the variability due to this selection of motor commands was minimized. The observed variability must therefore be mainly due to variability in movement execution (Schmidt et al. 1979). In contrast, a randomized design such as the one used by Gordon et al. (1994b) in which a target was never presented twice in succession might represent an additional computational load for the planning process and would therefore contain a relatively greater contribution of planning variability.

EXPERIMENT 2. Movements from a single starting position toward four targets in the same direction but at different distances (10.5, 21.0, 36.7, and 52.5 cm, see Fig. 1*B*) were tested. Subjects made each movement 60 times in a separate block for each target. Blocks were ordered with increasing distance, and they were separated by breaks of 1 min.

EXPERIMENT 3. This was a replication of *experiment 1* with some important methodological changes. The shoulder was restrained, and the subject's arm was fixed to a frictionless sled; therefore the hand moved in the horizontal plane only and did not touch the table. In addition, the starting position was defined by shoulder and elbow angles of 40 and 95°, respectively. The position relative to the right shoulder therefore differed across subjects; on average, it was 19 cm to the right and 12 cm in front of the starting position of *experiment 1*. Therefore comparable results between *experiments 1* and *3* would confirm some generalization across different postures, movement conditions, and subjects.

Prior to each experiment, subjects made one movement to each target to get accustomed to the procedure and the setup.

Kinematic analysis

We filtered the positional data of each individual movement with a second-order, zero phase-lag Butterworth filter with a 7 Hz cutoff frequency. Velocities were determined by numerical differentiation. The start of a movement was defined as the time the tangential velocity first exceeded 5 cm/s and remained above that until peak velocity. Movement end was defined as the first time after peak velocity the tangential velocity fell below 5 cm/s.

We used the same sets of recorded trajectories for the kinematic analysis and for the model simulations. To avoid sensitivity to occasional outliers within a set of trajectories, we rejected movements whose duration or start or end position differed by more than 3 SD from the mean of that set. We also rejected movements that exhibited multiple velocity peaks. In total, 2.7% of the trials were rejected.

To analyze the endpoint distributions, we determined for each subject and each target the covariance matrix of all the (nonrejected) two-dimensional end positions. These were visualized by 95% confidence ellipses. We calculated three parameters to fully describe each ellipse. First, the *aspect ratio*, calculated as the square root of the ratio of the two eigenvalues (the larger divided by the smaller) of the covariance matrix, is a measure of the shape of the ellipse. Second, we calculated the ellipse *orientation* as the orientation of the eigenvector corresponding to the largest eigenvalue. Finally, the *total variance*, the trace of the covariance matrix, expresses the mean squared distance from the mean. It equals the sum of the variances in (any) two orthogonal directions.

Because we were interested in the orientation relative to the movement direction, we calculated the *orientation deviation* as the difference between the ellipse orientation and the *overall movement direction*, defined as the orientation of the vector from the initial to the final position of a trajectory. Since this measure has a low reliability for distributions that are approximately circular, we multiplied it by (*aspect ratio* −1). This is equivalent to weighting each data value by its reliability. We also analyzed the variability in movement direction at the initial phase of movement. *Initial movement direction* was defined as the orientation of the vector between the positions at the 1st and 12th frame of a movement (i.e., 92 ms into the movement, at which moment approximately 1 cm had been traveled). The variability herein was quantified by calculating the circular SD (Fisher 1993).

Estimation of motor commands

Our aim was to verify whether the observed movement variability could have been caused by execution noise. We therefore determined the expected variability for observed movements by adding noise to their motor commands (see *Noise model*). As a first step, we needed to estimate the motor commands that had produced the observed movements before they had been corrupted by execution noise (see Fig. 2). To do this, we first derived mean trajectories for the movements toward each target for each subject in the following way. We used all 30 (*experiments 1* and *3*) or 60 (*experiment 2*) trajectories toward a target, apart from those that had been rejected because they deviated too much from the others (see *Kinematic analysis*). To avoid the possibility that the mean trajectory would be influenced by trajectories that deviated spatially from the others, i.e., because they were more curved, we selected the 50% most representative trajectories. This was done by choosing the median 50% movements in terms of their intersection with the perpendicular bisector of the starting and target positions. Next, the remaining trajectories were temporally rescaled to the mean duration, and their starting positions were aligned with the mean starting position. Finally, the trajectories were temporally resampled at 10 ms using linear interpolation. The means of these temporally resampled trajectories defined the mean trajectories.

The next step was to derive the motor commands from these mean trajectories. We followed the method used by Harris and Wolpert (1998); all the equations used are given in the APPENDIX. First, finger positions were transformed into joint angles (inverse kinematics), using the measured lengths of each subject's forearm and upper arm and assuming only movement at the shoulder and elbow joints. Joint angles were then transformed into joint torques using the inverse

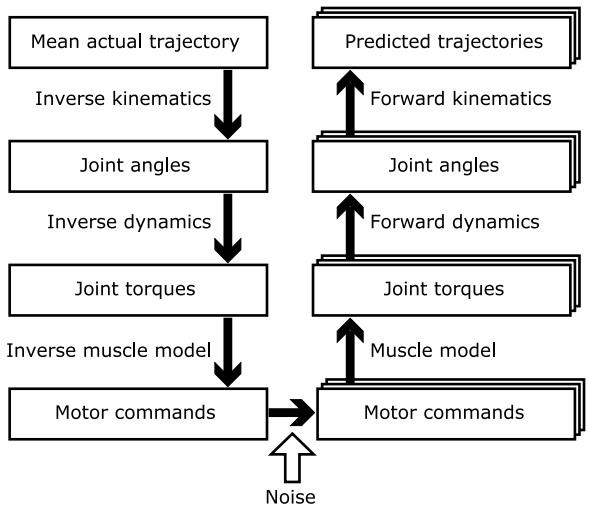

FIG. 2. Schematic representation of the execution noise model. *Left*: how motor commands are derived from the observed mean finger trajectory. Noise is added to 150 sets of these motor commands. *Right*: how the resulting finger trajectories are calculated from the sets of noisy motor commands.

dynamics equations for a two-link arm in the horizontal plane (e.g., Uno et al. 1989). The values for the mass, moment of inertia, and center of mass of each arm segment were taken from Kawato (1995) and scaled according to the actual lengths. The viscosity coefficient of both joints was set to 0.8 kg m^2/s (Nakano et al. 1999). Motor commands were calculated from joint torques assuming two second-order linear muscles acting on the shoulder and elbow joint with time constants of 30 and 40 ms, representing excitation and activation (van der Helm and Rozendaal 2000).

Noise model

We assume that the motor commands actually sent at a particular movement correspond to those derived above, corrupted by noise. We also assume that noise is added throughout the entire movement time. This corresponds to an open-loop control scheme. The role of feedback that could be used to reduce variability will be discussed in the RESULTS and DISCUSSION. Noise will cause the actual trajectory to deviate from the intended trajectory. To estimate the movement variability resulting from this noise, we simulated large numbers of noisy motor commands and calculated the corresponding trajectories by feeding them through the forward equations shown at the right side of Fig. 2.

There are many different types of noise that could be added to the motor commands. Since the motor commands have a time varying magnitude, we can add noise vertically, i.e., to the magnitude of the signal, as well as horizontally, i.e., in how the signal evolves over time. From the many types of noise possible, we included three types that have been proposed in the literature.

First, Harris and Wolpert (1998) proposed signal-dependent noise (SDN). This is white noise in the magnitude of the signal with zero mean and a SD proportional to the absolute value of the signal. Such a relation has been observed for both the firing of motor neurons (Pastor et al. 1991) and for force production during isometric contraction (Jones et al. 2002; Schmidt et al. 1979; Slifkin and Newell 1999). We modeled SDN by adding Gaussian white noise to the motor command at each time-step in the simulations. The SD σ_{SDN} of this noise was defined as $\sigma^2_{SDN} = k^2_{SDN}u^2$, where u is the motor command and k_{SDN} defines the level of the noise. Noise in the shoulder and elbow commands was assumed to be independent.

Second, noise could have a constant level independent of the signal (Wolpert et al. 1995). Constant noise could result from background activity of the motoneurons, but it could also represent the effects of other processes such as co-contraction (see DISCUSSION). We modeled constant noise (CN) in the same way as SDN, but with a SD independent of the motor command: $\sigma^2_{CN} = k^2_{CN}$. Constant and signal-dependent noise were assumed to be independent, so that the SD of the total amount of noise added to the magnitude of the motor commands was $\sigma_u = \sqrt{\sigma^2_{SDN} + \sigma^2_{CN}} = \sqrt{k^2_{SDN}u^2 + k^2_{CN}}$.

Finally, we added temporal noise (TN) to the motor commands to account for variability in movement time (M). The level of temporal noise was defined by the coefficient of variation of movement time, k_{TN}. Movement time was varied by changing the time-step in the forward calculations. All time-steps within a single simulated movement were scaled by the same factor, but this factor was varied across simulated movements to obtain a coefficient of variation of movement time of k_{TN}. Our data (see RESULTS) showed that movements with a longer duration tended to have a lower peak velocity. To account for this, we also scaled the magnitude of the motor command. Within a single simulated movement, movement time M and motor command u were scaled simultaneously such that when M was scaled by a factor c, u was scaled by a factor $1/c^2$ (Hollerbach and Flash 1982). This ensured that movements with a longer duration on average had a lower peak velocity (see RESULTS). The same scaling was applied simultaneously to the shoulder and elbow commands.

Fitting the model

We generated 150 sets of noisy motor commands for each target for each subject and calculated the resulting movement trajectories. The endpoint of a simulated movement was defined as the position immediately after the last motor commands had been sent (other methods, such as using a velocity threshold produced very similar results).

The simulations had three free parameters: the levels of the three types of noise (k_{SDN}, k_{CN}, k_{TN}). To estimate these noise levels, we fitted the model to the data of *experiment 1* by optimizing the log likelihood of the observed endpoints (Eliason 1993). This involved several steps. First, for a given set of noise levels, we simulated 150 movements for each target and each subject. We then fitted each set of 150 simulated endpoints to two-dimensional Gaussian distributions. These distributions defined the model predictions. We next computed the log likelihood for each observed endpoint given the corresponding predicted distribution, and we added these log likelihood scores together. This sum quantifies how good the observed endpoints match the predictions. The sum was optimized using an unconstrained nonlinear optimization algorithm (fminsearch in Matlab; The Mathworks, Natick, MA) that determined the three noise levels that produced the highest likelihood score. The same set of three parameters was used for all subjects and targets.

RESULTS

Experiment 1

CONSTANT ERRORS. Figure 3 shows the movement endpoints and the mean trajectories for a representative subject. This subject showed considerable overshoots for most movements in the 90–180° directions. This was not observed for other subjects. Subjects showed idiosyncratic constant errors, and no general pattern emerged. We therefore did not analyze the constant errors further but focused on the variability only.

ENDPOINT VARIABILITY. Figure 3 shows that the endpoint ellipses generally align with the movement direction. It is striking, however, that the ellipse shape varies with direction. For targets in the 22.5–45° directions (Fig. 3, *bottom left*), the ellipses are quite elongated. From 45 to 225°, they tend to be rounder, but between 225 and 270°, they are again more elongated. In the remaining directions, they are again rounder.

To see how general this effect is, we show in Fig. 4*A* the

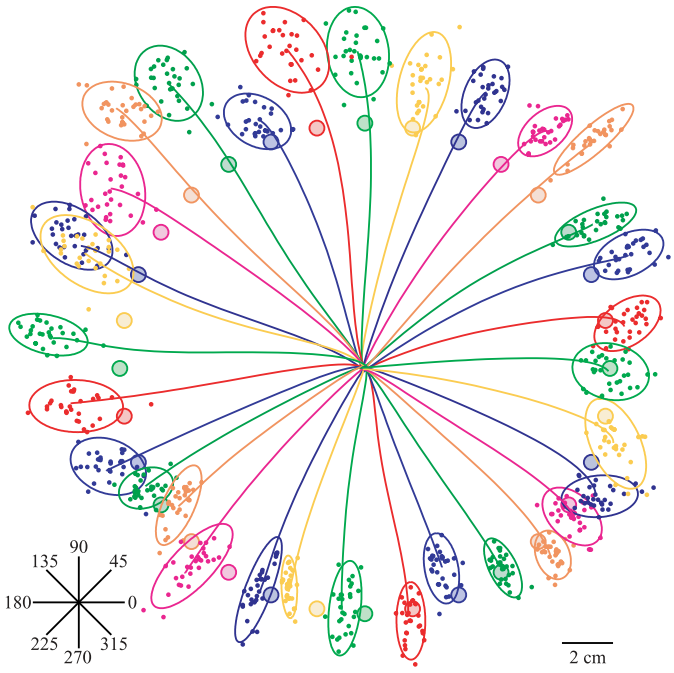

FIG. 3. Example of raw data of a representative subject (VL) in *experiment 1*. Large filled circles represent the 32 targets. Starting position (not shown) was in the center of the circle of targets. Curves emanating from this center represent the mean finger trajectories toward each target. Little dots around the end of the trajectories denote the endpoints of individual movements. Ellipses are 95% confidence ellipses of the endpoint distributions. *Bottom left*: target directions (in °) are defined.

aspect ratio averaged over all subjects as a function of target direction. This plot confirms that the aspect ratio varies with direction. It has maxima near the 56 and 247.5° directions, where it reaches values around 3. The value in most other directions is about one-half this peak value. We used Moore's modification of Rayleigh's test (Moore 1980) to verify whether the aspect ratio (and other quantities as well) varies significantly with direction. This test evaluates whether directional data could have been drawn from a uniform circular distribution. This test, here assuming a bimodal circular distribution as the alternative for uniformity, confirmed that the aspect ratio varies with direction ($R^*_{(320)} = 1.536$; $P < 0.001$).

Figure 4*B* plots the mean orientation deviation (the ellipse orientation relative to the overall movement direction). This figure shows that the ellipses are approximately aligned with the movement direction, in accordance with the findings of Gordon et al. (1994b). However, the orientation deviation varies weakly but significantly with direction ($R^*_{(320)} = 1.182$; $P < 0.025$). The mean total variance is plotted in Fig. 4*C*. The total variance does not significantly ($R^*_{(320)} = 0.527$; $P > 0.4$) vary with direction, and its mean is 68 mm^2.

VARIABILITY IN INITIAL MOVEMENT DIRECTION. Figure 4*D* shows the mean of the reciprocal of the circular SD in the initial movement direction. Clearly, this variability early in the movement varies with movement direction ($R^*_{(320)} = 2.114$; $P < 0.001$) in a similar way as the aspect ratio does. This suggests that these measures could be related and that an indication of the endpoint variability may already be visible in the earliest parts of the movements. To test for this possibility we tested whether, within a block of movements to the same target, the initial and overall movement direction are correlated. Since these are both directional data, we calculated the angular-angular correlation (the analogue of the correlation coefficient, see Zar 1999). The mean angular-angular correlation was 0.34, and the correlation was significantly greater than zero in 285 of 320 (10 subjects × 32 targets) cases (89.0%). We also tested whether a similar relation exists between the distance traveled within the first 12 frames and the final movement extent. Here the mean correlation coefficient was 0.20, and it was significantly greater than zero in 110 of 320 cases (34.4%). This confirms that some aspects of the endpoint variability, mainly the directional variability, are already present in the earliest part of movement (see also Messier and Kalaska 1999). The correlations are, however, rather weak, which suggests that a substantial part of the endpoint variability is due to noise that is added after the initial movement phase and/or that there is compensation for the variability in the beginning of the movement.

TEMPORAL VARIABILITY. Movement times were variable. Figure 5*A* shows the mean movement time as a function of movement direction. Mean movement time varied in a systematic way with direction, with extremes of 374 and 487 ms. Such an effect has previously been reported by Gordon et al. (1994a). These authors attributed this effect to the nonuniform inertia experienced when moving the hand in different directions. To verify this, we also plotted the inertia (derived from the inverse of the mobility tensor, see Hogan 1985) averaged across subjects (the dashed line in Fig. 5*A*). Movement time clearly increases with inertia. Tangential velocity profiles showed the well-known bell-shaped pattern, and did (after normalization in magnitude and time) not vary with direction

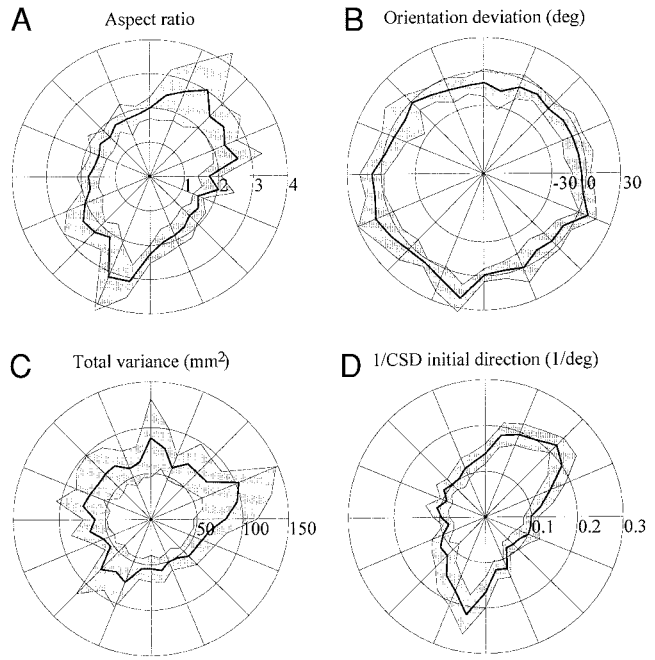

FIG. 4. Polar plots of observed endpoint variability in *experiment 1*. In each plot, the black curve shows the mean of all subjects as a function of target direction, and gray areas around it represent intersubject variability (1.96 times the SE, i.e., the 95% CI). *A*: aspect ratio of endpoint ellipses. *B*: orientation deviation of endpoint ellipses: scaled difference between the ellipse orientation and overall movement direction. *C*: total variance in movement endpoints. *D*: reciprocal of the circular SD (CSD) in initial movement direction.

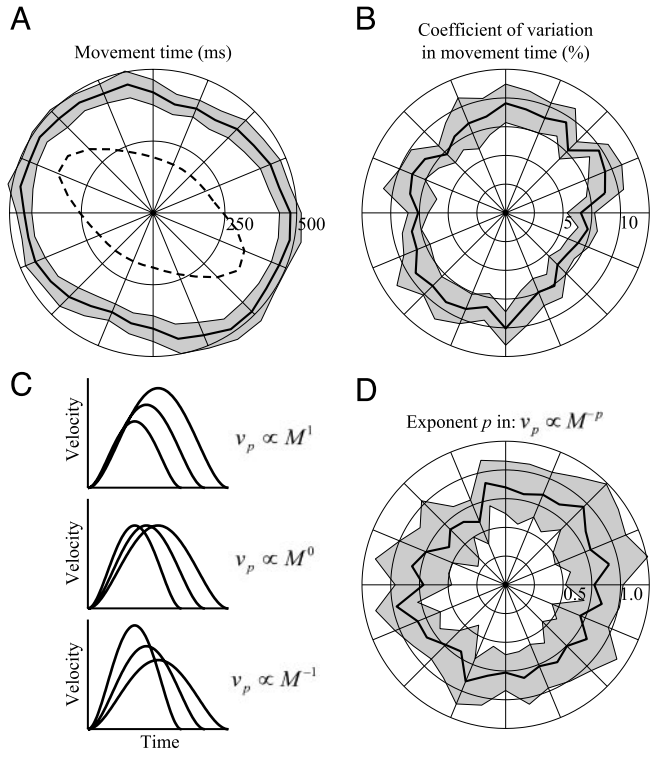

FIG. 5. Temporal variability. The format of the polar plots is the same as in Fig. 4. *A*: mean movement time. The dashed line indicates inertia as a function of movement direction (in arbitrary units). *B*: coefficient of variation in movement time. *C*: 3 examples of possible relations between movement time M and peak velocity v_p for 3 movements to the same target with different movement times. *D*: polar plot of the observed exponent p in $v_p \propto M^{-p}$.

[data not shown, but see Gordon et al. (1994a) and Messier and Kalaska (1999) for similar data].

Figure 5*B* shows the coefficient of variation (the SD divided by the mean) in movement time. This coefficient does not vary with direction ($R^*_{(320)} = 0.520$; $P > 0.4$) and has a mean value of 0.084. The key question about the variability in movement time is whether it is related to spatial variability. Do faster movements follow the same path as slower movements or are their paths different? Since the normalized velocity profile is approximately constant, we can address this question by analyzing the relation between movement time and peak velocity v_p. To get the idea behind this analysis, consider the schematics plotted in Fig. 5*C*. These diagrams represent three possible relations between peak velocity and movement time for three movements to the same target with different movement times. In the first, peak velocity increases with movement time. This would result from producing torques of the same magnitude for all durations by only scaling the torque profile in time. As a result, movement amplitude, which is proportional to the product of peak velocity and movement time, will be proportional to the square of movement time. A second possibility, shown in the middle, is that peak velocity is independent of movement time. This could be accomplished by appropriate scaling of the torque magnitude. In this case, amplitude is proportional to movement time. A third possibility, shown at the bottom, is that peak velocity is inversely proportional to movement time so that the amplitude is independent of movement time. This means that the spatial path is the same for all movement times, only the speed is varied. Of course, these three possibilities are just three points on a continuum of possible relationships. The continuum can be described by the relation $v_p \propto M^{-p}$, where power p defines the relationship.

We determined p by performing linear regressions of $\log(v_p)$ as a function of $\log(M)$ for each target and subject. Figure 5*D* shows the mean value of p as a function of direction. The mean value is 0.80, and it does not vary with direction ($R^*_{(320)} = 0.144$; $P > 0.9$). This implies that movements with a longer duration tend to have a lower peak velocity. Since the value of p is slightly smaller than 1, however, the effects of duration and velocity do not cancel completely; therefore, on average, movement extent increases slightly with movement time.

This result forms the basis for how we modeled temporal noise. The observed relation between movement time and peak velocity suggests that motor commands are scaled down with increasing movement time. Hollerbach and Flash (1982) showed that a scaling of movement time M by a factor c is accomplished by scaling the joint torques by a factor $1/c^2$. However, the dynamics of the arm considered by these authors contained inertial terms only and not the viscous terms we incorporated in our arm model. Also, our model adds noise to motor commands, not to torques. Since these differences are not expected to have large effects and since the observed exponent p was quite close to 1, we modeled the temporal variability by a simultaneous scaling of movement time and motor command magnitude according to the relationship derived by Hollerbach and Flash (1982) (see METHODS).

MODEL PREDICTIONS. The analysis of the variability in movement endpoints and in initial movement direction showed that movement variability varies systematically with movement direction. We next examined whether these results can be explained by noise in movement execution. Our execution noise model contains three types of noise. We will now demonstrate the effect of each of these types of noise.

The *top row* of Fig. 6 shows the effects of signal-dependent noise. Figure 6*A* shows the predicted endpoint ellipses for the subject whose data are shown in Fig. 3, and Fig. 6*B* shows the aspect ratio averaged across all subjects. The predicted aspect ratios are, in general, too large. However, it is interesting to note that the predicted and the observed aspect ratios reach their maxima for approximately the same movement directions. The maxima correspond to directions for which the torques and motor commands at one of the joints are small compared with those at the other. The noise at one of the joints will therefore be much larger than at the other, which leads to highly elongated ellipses. The ellipse orientation, however, is not well predicted. In the 90–180° directions, for instance, the predicted ellipses are approximately orthogonal to the observed ones. In these directions, torques have to be generated at both joints. These torques work in different directions, so that their effects cancel partially. Their noises, however, add. The result is a larger variability orthogonal to than along the movement direction.

The predictions for constant noise are shown in the *middle row* of Fig. 6. Here, the ellipse orientation does not vary much with direction, and the aspect ratio is approximately constant. Since this noise is independent of the motor commands, the ellipses are hardly influenced by the movement made. They resemble the ellipse that would be found when constant noise is added to a stationary arm. Only the ellipse size varies with

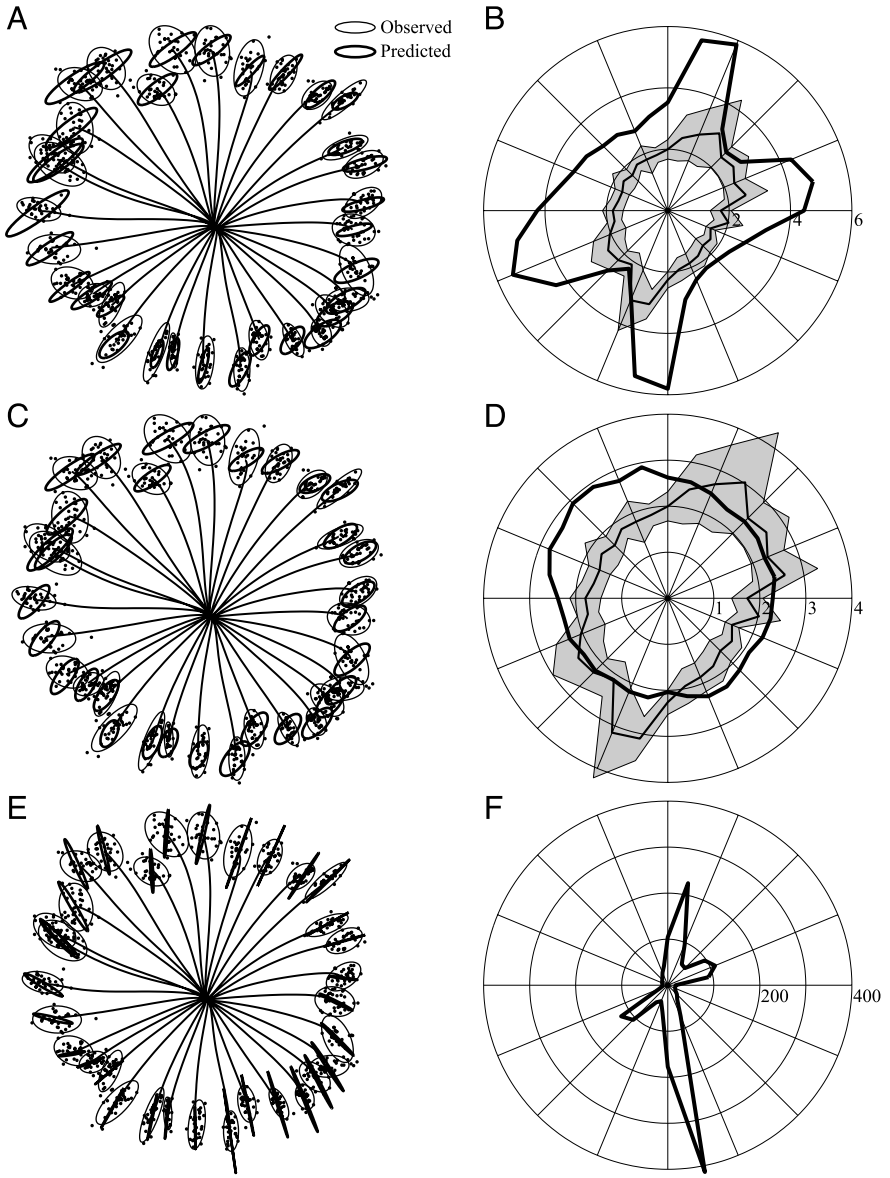

FIG. 6. Endpoint variability resulting from each type of noise included in model. *Left*: endpoint ellipses for the subject whose data are shown in Fig. 3. Predictions are shown as thick black ellipses. *Right*: observed and predicted aspect ratio averaged across all subjects. The format is the same as in Fig. 4, apart from the thick black line that represents the prediction. *A* and *B*: only signal-dependent noise ($k_{SDN} = 0.2$). *C* and *D*: only constant noise ($k_{CN} = 0.2$). *E* and *F*: only temporal noise ($k_{TN} = 0.08$).

direction. This is because the movement time, and therefore the amount of noise added, depends on direction (Fig. 5*A*).

Temporal noise (Fig. 6, *bottom row*) leads to much more variability in the movement direction than orthogonal to that. The predicted aspect ratio is therefore orders of magnitude too large. Temporal noise alone thus leads to variation of movement extent with movement time, as we found experimentally.

None of the three types of noise in isolation can account for the observed endpoint variability. We next examined whether a combination of the three types of noise can explain the data. We fitted the model containing all three types of noise to the data (see METHODS). The only free parameters were the three noise levels, and these were assumed to be the same for all subjects and targets. The best fitting parameters were $k_{SDN} = 0.103$, $k_{CN} = 0.185$, and $k_{TN} = 0.083$.

Figure 7 shows the predicted endpoint variability for the subject whose data are shown in Figs. 3 and 6. This model captures the observed endpoint variability much better than the models including only one type of noise. To determine whether the improvement is better than that expected from the increase of degrees of freedom from one to three, we determined Akaike's information criterion (AIC; Akaike 1973) for each model using the data from all subjects. The AIC is a measure for the quality of the model fit, based on the likelihood, that includes the model's degrees of freedom. This measure thus allows an objective comparison of models with different degrees of freedom; the lower the AIC, the better the model. Table 1 shows the AIC for all versions of the model, i.e., all possibilities including one, two, or three types of noise. The AIC for the model with three types of noise is the lowest. This suggests that all three types of noise are essential to include in the model. Therefore our further analyses focused on the three component model only.

Figure 8 compares the predicted and observed variability averaged across all subjects. The variation of the aspect ratio with movement direction is predicted very well (Fig. 8*A*). The location and magnitude of the predicted maxima agree with the observed ones. These predictions are significantly better than those of any model predicting a constant aspect ratio (paired *t*-test on squared differences between observed and predicted

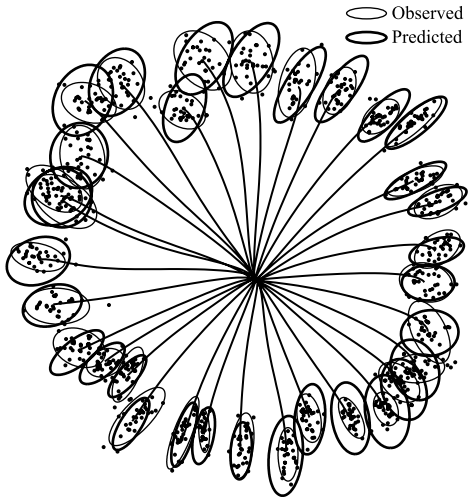

FIG. 7. Example of predicted endpoint variability for a representative subject (VL) in *experiment 1*. The model including all 3 types of noise (see RESULTS) is used to predict the endpoint variability for the subject whose data are shown in Fig. 3.

aspect ratio: $P < 0.05$). The ellipse orientation (Fig. 8*B*) is also predicted reasonably well. Although the predicted magnitude of especially negative orientation deviations is slightly too large, the sign of the deviation is usually predicted correctly. Finally, the model prediction for the total variance (Fig. 8*C*) is not as good. Although the prediction is correct in about one-half the directions, it is too large in the 90–180° and especially in the 270–360° directions. This is also evident in the example in Fig. 7.

A possible explanation for the poor prediction of the variance is that there is compensation for variability that occurred early in the movement. Such corrections are not included in the model but will naturally reduce variability. Corrections must have been based on proprioceptive feedback because subjects could not see their arm. The mean movement time of 420 ms is sufficiently long to allow for such corrections (see DISCUSSION). However, movement time varied with direction (Fig. 5*A*). The directions in which the predicted variance is too large correspond to those with a long movement time (compare Figs. 8*C* and 5*A*). The mean movement time varied between 374 and 487 ms; any such difference of over 100 ms could certainly be important in determining to what extent feedback-driven corrections might occur. This suggests that the poor prediction of the variance could indeed be caused by compensation for

TABLE 1. *AIC values for the model including different types of noise*

Noise Included	AIC
SDN	−133477
CN	−135684
TN	−23899
SDN + CN	−137829
SDN + TN	−135792
CN + TN	−142024
SDN + CN + TN	−142108

The AIC values for each version of the model were determined by optimizing the likelihood by varying the levels of the included types of noise. The levels of the types of noise that were not included were set to zero. AIC, Akaike's information criterion; SDN, signal-dependent noise; CN, constant noise; TN, temporal noise.

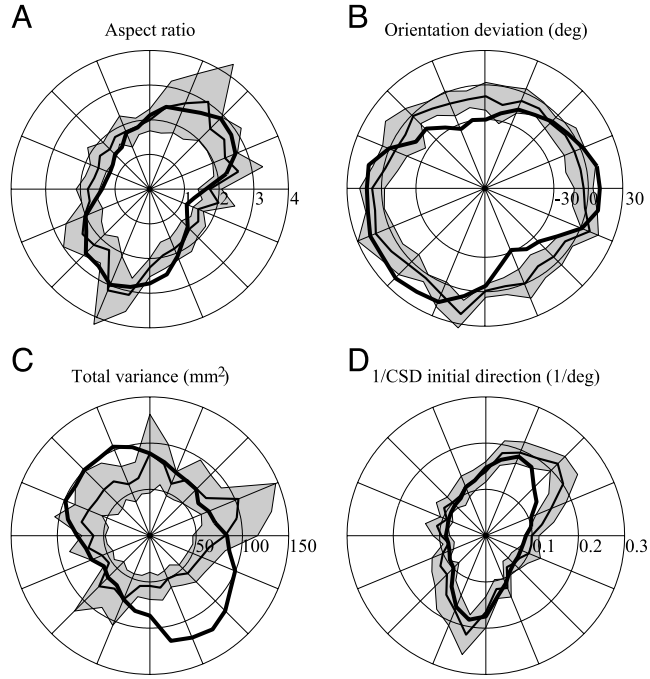

FIG. 8. Polar plots of observed and predicted variability in *experiment 1*. Observed values are plotted in the format of Fig. 4. Model predictions, with the 3 noise levels optimized (see RESULTS), averaged across all subjects, are indicated by thick black curves. *A*: aspect ratio. *B*: orientation deviation of endpoint ellipses. *C*: total variance. *D*: reciprocal of the circular SD in initial movement direction.

variability earlier in the movement. If this were the case, the model predictions should still be correct earlier in the movement. Figure 8*D* shows the observed and predicted variability in initial movement direction. This figure confirms that the variability in the initial part of the movement is predicted very well. We next investigated how far into the course of the movement the predictions agree with the observations. Figure 9 plots the observed and predicted total variance at 200, 250, 300, and 350 ms into the movement. Observed and predicted variance agree very well until 250 ms into the movement. At 300 ms they begin to differ, and at 350 ms they differ strongly, almost to the extent that the variances in the endpoints differ (cf. Fig. 8*C*). Thus although we fitted the model to the observed endpoints only, it makes an excellent prediction for the variability in the initial part of the movement. The model is less successful at fitting the variability at later times in the movement; total variance increases less rapidly than the model predicts after 250 ms. This suggests an additional control process comes into operation beyond 250 ms to reduce variability. Our data are consistent with the possibility that feedback-driven corrections become effective around 250 ms after movement onset.

Experiment 2

Experiment 1 showed that movement variability varies with movement direction. We showed that noise in movement execution can explain these results. In our execution noise model, variability in movement extent is to a large extent caused by temporal noise. The results of *experiment 1*, however, do not provide evidence that variability in movement extent is actually caused by temporal noise and not by noise in planning of

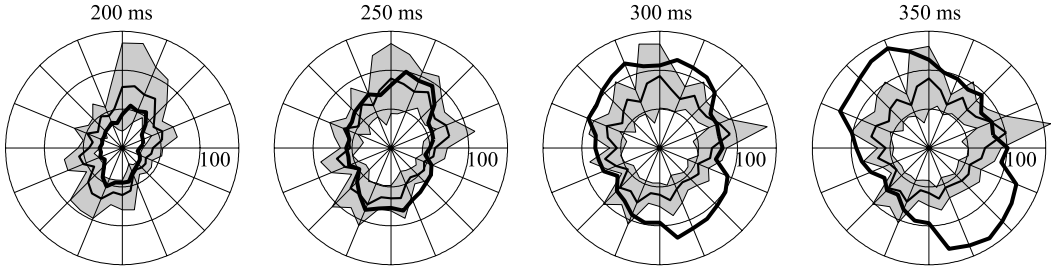

FIG. 9. Polar plots of observed and predicted total variance in the finger position during the movements in *experiment 1*. The format is the same as in Fig. 8. Times above plots indicate at which moment after movement onset the variance is shown.

movement extent. We performed *experiment 2* to distinguish between these possibilities. Subjects again made arm movements toward visual targets, but this time we used longer movements in a direction where it is known that finger trajectories are curved (Desmurget et al. 1997; Haggard and Richardson 1996). Curved trajectories can distinguish between the two possibilities. According to the movement planning vector hypothesis (Gordon et al. 1994b), the movement's endpoint is chosen before the trajectory or motor commands are determined. Variability in the planned extent will thus result in variability along the (straight) vector from starting to end position. After that, the trajectory and motor commands will be determined that will bring the hand to the selected movement endpoint. Whether or not the trajectory is curved is not relevant for the endpoint variability since the endpoint variability is fully determined during planning of the movement vector, according to this hypothesis. The movement planning model thus predicts variability along the straight line from starting to end position, regardless of trajectory curvature. In contrast, the effect of noise in movement execution will depend on the trajectory, so that the endpoint variability is likely to vary with trajectory curvature. Jaric et al. (1999) earlier reported that highly curved movement trajectories, induced by placing an obstacle between starting and target position, influenced the orientation of the endpoint ellipses. Their study, however, did not make clear whether this effect was caused by the curved trajectories per se, or to the fact that their subjects produced a series of submovements, each of which was planned independently.

ENDPOINT VARIABILITY AND TRAJECTORY CURVATURE. Figure 10 shows the mean trajectories and movement endpoints for a representative subject. The movements toward the near targets were approximately straight, but those to the two furthest targets were clearly curved away from the body. We quantified the curvature by determining the linearity index (Atkeson and Hollerbach 1985): the maximum distance of the finger trajectory from the straight line between start and end position, divided by the length of this straight line. Curvature away from the body was positive, curvature toward the body was negative. Across all subjects, movements toward all but the nearest target had a significantly positive linearity index (2-tailed *t*-test, all $P < 0.02$). In addition, curvature increased with movement distance (mean correlation coefficient: 0.90, significant for 6 of 7 subjects). In contrast to the study of Jaric et al. (1999), these movements were "naturally" curved and planned as single movements, as is evident from their single-peaked velocity profiles (data not shown).

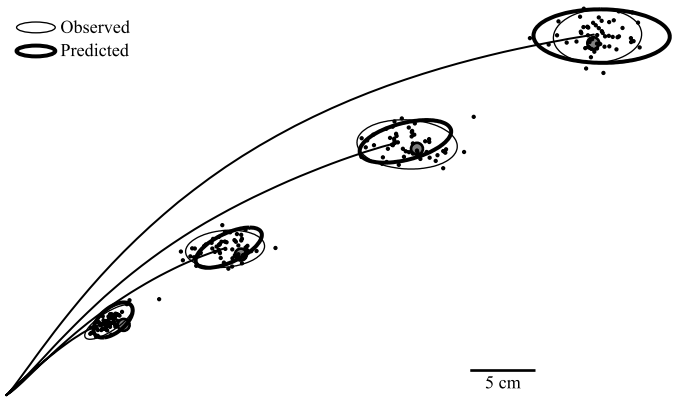

FIG. 10. Example of raw data of a representative subject (SY) in *experiment 2*. Large filled circles represent targets. Curves represent mean finger trajectories toward each target. Endpoints of individual movements are shown as little dots. Thin ellipses are 95% confidence ellipses of endpoint distributions. Thick ellipses represent predictions of the execution noise model.

For the nearest target, which was at a similar distance as the targets in *experiment 1*, the ellipse in Fig. 10 is approximately aligned with the overall movement direction. This is, however, not true for the further targets. Here, the ellipse orientation deviates from the orientation of the straight line between initial and final position. The deviation is in the direction of movement curvature. Figure 11*A* plots the ellipse orientation deviation as a function of target distance. The orientation deviation is significantly greater than zero for the two furthest targets (1-tailed *t*-test, both $P < 0.025$) but not for the two nearest targets. The aspect ratio (Fig. 11*B*) decreases slightly with target distance, in agreement with findings of Gordon et al. (1994b). The total variance (Fig. 11*C*) increases with target distance.

MODEL PREDICTIONS. The finding that the ellipse orientation deviates from the overall movement direction for curved trajectories suggests that the variability in movement amplitude is not due to variability in the planned length of the vector from initial to final position. Note that also a planning model that plans straight trajectories, but that produces curved movements because of inaccuracies in the planning process, cannot explain this result. Desmurget et al. (1997) tested movements very similar to ours, and found that these were naturally curved. However, when instructed to make the same movement following a straight-line path, subjects produced much straighter trajectories. This suggests that the movements in our experiment were planned to be curved and that the orientation of the endpoint ellipses does not result from inaccuracies in planning that adds curvature to movements that are intended to be straight. Does our model of execution noise predict these ellipse orientations correctly? We used the same model as in *experiment 1*, including the optimal noise levels determined there, to predict the movement variability in these movements. We made two modifications. Numerous studies on temporal variability (e.g., Ivry and Hazeltine 1995; Wing and Kristofferson 1973) have found that the coefficient of variation in the

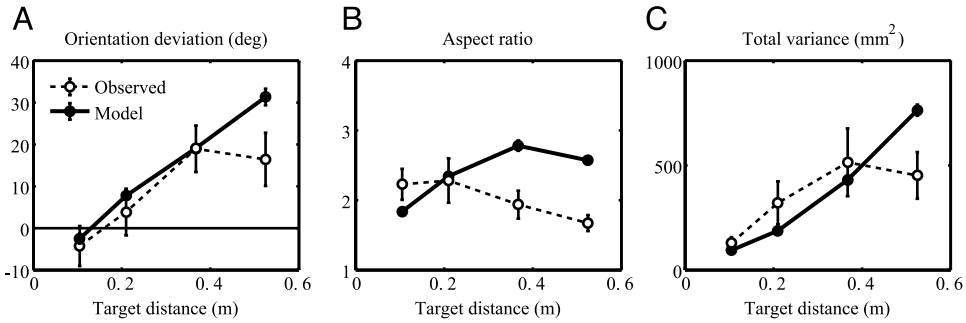

FIG. 11. Observed and predicted endpoint distributions in *experiment 2*. Mean values represent the mean across all subjects. Error bars denote SE reflecting inter-subject variability. *A*: orientation deviation of endpoint ellipses: difference between the ellipse orientation and overall movement direction. *B*: aspect ratio. *C*: total variance.

duration of tapping intervals decreases with the length of the interval. Since the movement time in this experiment varied, we allowed this coefficient of variation in the model (k_{TN}) to decrease with movement time. We fixed k_{TN} at the mean movement time of *experiment 1* (420 ms) at the value used there (0.083) and let it linearly decrease with movement time to 0.05 at the mean movement time at the furthest target (750 ms). In addition, the furthest targets were much further in front of the subject than the targets in *experiment 1*. Because visual localization uncertainty increases with distance from the observer (van Beers et al. 1998), it was no longer legitimate to neglect the uncertainty in target localization. We translated the reported estimate of visual localization precision of 0.5° arc (Hansen and Skavenski 1977; van Beers et al. 1998) into uncertainty on the tabletop and added this to the variability resulting from execution noise.

The predictions of this model are shown in Figs. 10 and 11. Most importantly, the predicted orientation deviation (Fig. 11*A*) increases with target distance and thus with trajectory curvature, just as the observed orientation deviation does. The predicted aspect ratio (Fig. 11*B*) differs somewhat from that observed but the differences are relatively small. The total variance (Fig. 11*C*) is predicted reasonably well. Only for the furthest target are the predicted values somewhat too large. The discrepancies for this target are presumably due to compensation for variability early in the movement, as in *experiment 1*. If this were the case, the correlation between initial and overall movement direction would be expected to be lower for this target than for the nearer targets. This was indeed the case: whereas the mean angular-angular correlation was between 0.25 and 0.27 for the three nearest targets, it was only 0.03 for the furthest target. This confirms that the discrepancies between observed and predicted variability for the furthest target could have arisen from corrections for variability early in the movement.

Experiment 3

Experiment 3 was a replication of *experiment 1* with some methodological changes. First, air-sleds were used to allow subjects to move without any friction. This makes especially the end of the movement different from in *experiment 1*, where the movement endpoints could have been influenced by the friction encountered when the finger made contact with the table. Second, the shoulder was securely fixed to allow us to control for the effect of possible small shoulder movements. Third, movements were made in a different part of the workspace, and finally, different subjects were tested. These differences allowed us to test the generalization of the model across different postures, movement conditions and subjects.

Figure 12 shows the variability observed in this experiment. As expected, the peaks for the aspect ratio (Fig. 12*A*) and the variability in initial movement direction (Fig. 12*D*) occur for different target directions than in *experiment 1*. The figure also shows the values predicted by the execution noise model with the noise levels determined in *experiment 1*. Most importantly, the locations of the peaks are predicted correctly. The ellipse orientation (Fig. 12*B*) is also predicted accurately. In contrast to *experiment 1*, the predicted total variance (Fig. 12*C*) is smaller than the observed variance. This is due to two subjects who showed much larger variability than the subjects in *experiment 1*, possibly because they had no experience with the somewhat unnatural conditions with air-sleds. The other two subjects, who had been tested in this setup before, showed a variability comparable to that found in *experiment 1*. This can explain the large observed total variance and inter-subject variability therein. The patterns of observed and predicted total variance as a function of movement direction, however, are similar as in *experiment 1*: the observed total variance does not vary much with direction, whereas the predicted variance is larger in directions where movements had a longer duration.

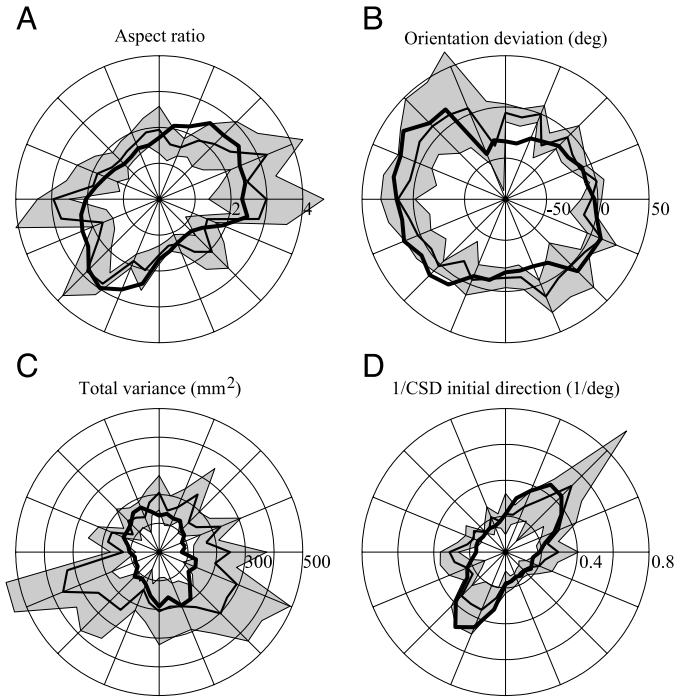

FIG. 12. Results of *experiment 3*. Mean observed and predicted values are shown in the format of Fig. 8. *A*: aspect ratio. *B*: orientation deviation of endpoint ellipses. *C*: total variance. *D*: reciprocal of circular SD in initial movement direction.

Taken together, the results of this experiment are in good agreement with the model predictions. This suggests that possible small movements of the shoulder and friction at the end of the movements in *experiment 1* had little or no influence on the observed variability. In addition, the fact that the model works equally well in a different part of the workspace and for different subjects illustrates its predictive power.

DISCUSSION

We have investigated the role of execution noise in movement variability by analyzing the variability in arm movements to visual targets without visual feedback of the arm. The experimental conditions minimized the variability caused by movement planning and by uncertainty in hand and target localization. Our experiments produced two novel findings. The first and third experiment showed that the variability in movement endpoints and in initial movement direction varies systematically with movement direction. The second experiment showed that the endpoint distributions of movements with curved finger trajectories are not aligned with the straight line between initial and final finger position, but they are rotated in the direction in which the trajectory is curved. These results are well accounted for by a model that assumes that the variability is due to noise in movement execution, which is a combination of signal-dependent and signal-independent noise in the magnitude of motor commands and temporal noise in their duration. The model has a large predictive power, because it was only fit to the movement endpoints in one experiment, but it also captures the variability at earlier times in these movements as well as the variability in movements of different extents and in other parts of the workspace. The execution noise model is a parsimonious model because it does not make any ad hoc assumptions; it only assumes noise in the magnitude and duration of motor output, the existence of which is beyond doubt.

It has been shown previously that the variability in arm movements of deafferented patients varies with direction (Ghez et al. 1990). Buneo et al. (1995) suggested that this effect might be the result of random variability in the magnitude of joint torques. We went one step further by showing that the movement variability in healthy humans also varies with direction. Furthermore, using a more realistic model for noise in movement execution than Buneo et al. (1995) used, we showed that this noise can explain the observed movement variability in healthy humans. Earlier models for one-dimensional movements (Meyer et al. 1988; Schmidt et al. 1979) also attributed movement variability in healthy humans to noise in both the amplitude and the duration of motor output. However, whereas the motor system in these earlier models was modeled as a black box with input-output relations based on empirical relationships between task parameters and observed variability, our model has a "mechanistic" base that models the torques and neural signals that are actually present and in which it is made explicit where the noise arises. Our model is therefore more realistic, makes stronger quantitative predictions, and has a larger generality than these earlier models.

Possible other sources of variability in our data

Although the observed variability is well explained by noise in movement execution, we have not yet shown that it does not include substantial variability arising at the localization and planning stages. It is impossible to completely exclude any such contributions, but we have several reasons to assume that these are unlikely to be large.

First, the experimental conditions minimized the localization and planning contributions. The localization contribution was minimized because the targets were well visible during pointing in a structured visual field (Conti and Beaubaton 1980) and subjects could simultaneously see their hand (Desmurget et al. 1995) and the target (Rossetti et al. 1994) before each movement. Visual localization precision has been estimated to be better than 0.5° arc (Hansen and Skavenski 1977; van Beers et al. 1998). For the target positions used in *experiments 1* and *3,* this corresponds to a variance smaller than 20 mm^2. This is small compared with the mean endpoint variance of 68 mm^2 in *experiment 1*. The effect of hand localization will be much smaller because both vision and proprioception provided information (van Beers et al. 1996, 1999). The contribution of movement planning was minimized because a blocked design was used in which subjects pointed to the same target many times in succession. This allowed subjects to refine their movements and thus the motor commands they sent to their muscles. In this situation, noise in motor output is likely to be the major source of variability (Schmidt et al. 1979).

The second reason why the contributions of localization and planning must be small is that they cannot explain the direction-dependent variability we found in the center-out experiments. Localization of a visual target is limited by how precise the orientation of the eyes is sensed (Hansen and Skavenski 1977). Translated into uncertainty on the tabletop, this results in ellipses whose major axes point toward the eyes. The ellipses we found clearly had a different orientation. The effect of hand localization on ellipse orientation will be smaller because the variance in localization of a seen hand is smaller than that of a visual target (van Beers et al. 1996). Variability due to planning is also unlikely to vary with direction in the way our data do. The expected variability depends on the model for movement planning that is supposed. The model of Gordon et al. (1994b) assumes independent variability in the planned direction and extent, and both are not assumed to vary with direction. This model thus does not predict the aspect ratio to vary with direction. An alternative planning model in which movements are not planned in external but in joint space might be able to produce direction-dependent variability. However, the combination of noise in the amplitude and in the duration of motor output, which we have shown to be necessary to explain the results and which makes sense for an execution noise model, does not seem a logical assumption for a planning model. We conclude that most of the variability we observed is caused by noise in movement execution.

Noise in movement execution

We will now discuss some important aspects of the execution noise model in more detail. In the model we added noise to motor commands, i.e., to the input to the muscle. However, previous data show that noise in muscle output arises from a combination of renewal process noise on the motoneurons and the recruitment properties of motor units (Jones et al. 2002). We therefore examined whether adding noise to the output of the muscles, i.e., to torques, instead of to their input, would

produce different results. The results (data not shown) were virtually unchanged, which suggests that the observed variability comes from the elements of the motor hierarchy (as shown in Fig. 2) common to both these simulations, namely the dynamics and kinematics of the arm. Thus movement variability varies with direction and trajectory curvature because the motor commands and torques do so, due to the kinematics and dynamics of the motor apparatus.

We next discuss the relative importance of the three types of noise (signal dependent, constant, and temporal noise) we found by fitting the model to the endpoints of *experiment 1*. The level of temporal noise is directly related to the observed variability in movement time. The fact that the optimal level of temporal noise (0.083) is almost identical to the observed coefficient of variation in movement time (0.084) confirms that this noise is modeled correctly. The exact levels of the noise in the magnitude of the motor commands are not so easy to interpret because they depend on the time-step used in the simulations (they scale with the reciprocal of the square root of the time-step). We can however interpret their relative values. The coefficient of constant noise (0.185) is larger than that of signal-dependent noise (0.103). Moreover, the average motor command level is of the order of 0.5 (in arbitrary units), with a mean peak of 1.25. Therefore multiplying even the peak motor command by the signal-dependent noise coefficient produces a noise level below that of constant noise. This suggests that the contribution of signal-dependent noise to overall variability is lower than that of constant noise. This is somewhat surprising, but it does not necessarily mean that actual motor commands have so much constant noise. One possibility is that the noise increases with the signal, but not as strongly as we assumed in our definition of signal-dependent noise. It seems likely that our model would approximate such noise by a combination of constant and signal-dependent noise. Another possibility is that the high level of constant noise is the effect of co-contraction. Our model contains highly simplified linear muscles that, to simulate agonist–antagonist pairs of muscles, can pull in two directions. Actual torques are produced by combinations of mono- and multi-articular muscles, each having their own noise. Coactivation of antagonistic muscles results in a partial canceling of their torques but at the same time their noises add up. Even if the noise in two co-contracting muscles is fully signal-dependent, the noise in the produced torque will be larger than when a single muscle produces the same net torque. Co-contraction thus raises the noise level so that the overall noise can be considered as a combination of signal-dependent and constant noise. Since co-contraction occurs naturally during movements from the first instants of muscle activation (Suzuki et al. 2001), at least a part of the constant noise appearing in our model will in fact be due to signal-dependent noise in co-contracting muscles. It is unclear, however, how large a part of the constant noise this is, because the level of cocontraction during movement is not known and because the increase of limb stiffness induced by cocontraction can also act to reduce positional variability (Gribble et al. 2003).

It is often instructive to identify what aspects of behavior a model fails to capture. Since our model is an open-loop model only, describing the failures of our model may have the positive role of isolating the contribution of sensory feedback in the control of aimed movement. Sensory feedback can be used to compensate for undesired deviations from an intended trajectory, thus reducing variability (Todorov and Jordan 2002; Woodworth 1899). Our subjects could not see their hand; therefore any corrections in their movements must have been based on proprioceptive feedback. Earlier estimates of the time for proprioceptive feedback to be effective are between 100 and 200 ms (Chernikoff and Taylor 1952; Cordo 1990; Cordo et al. 1994; Newell and Houk 1983; Vince 1948). Our model captures the variability until approximately 250 ms into the movement (Fig. 9). Thereafter the predicted variance exceeds the observed variability. This suggests that it takes about 250 ms before proprioceptive signals can induce corrections of the movement trajectory. The actual delay, however, may be shorter; the trigger signal for a correction would presumably be some deviation from the desired trajectory, which would occur at some unknown time after movement onset. Thus our data are not incompatible with the lower estimates of feedback delay measured by others.

General role of execution noise

We created experimental conditions in which the effects of localization and planning on movement variability were minimized. In other, more natural conditions, however, localization and planning could cause more variability. To judge the importance of execution noise, we must compare the variability due to execution noise to the variance that could be expected from the other sources.

As mentioned before, the variance expected from target localization uncertainty in our experiments is small compared with the variance due to execution noise. However, in general, this depends on the location of the target; the effect will be larger for targets further away. For the furthest target in *experiment 2*, for instance, an uncertainty of eye orientation of 0.5° arc (Hansen and Skavenski 1977) corresponds to a variance >150 mm^2. This is why it was included in the model for this experiment. The effect of uncertainty in hand localization depends on whether the hand can be seen. When it is seen, both vision and proprioception are used, so that its localization variance is much smaller than that of the target (van Beers et al. 1996, 1999). When the hand is not seen its position has to be derived from proprioception only, which is not so precise (van Beers et al. 1998). This explains why movement variability is larger when the hand is not seen before the movement than when it is (Desmurget et al. 1995).

The variance due to movement planning can be estimated by comparing the variance in our study to the variance found in a similar experiment in which the effect of planning was not minimized, i.e., an experiment in which the targets were presented in a random order. Most suitable for this comparison is task 1 in the study by Messier and Kalaska (1997). We derived the endpoint variance from the absolute variable errors they reported (their Fig. 4, *A* and *B*) at the target distance in our *experiment 1*. A conservative estimate reveals that the variance in the study of Messier and Kalaska was at most 90 mm^2. This is only marginally larger than the 68 mm^2 we found in *experiment 1*. This shows that the variability due to movement planning is small compared with the variability caused by execution noise. It further suggests that much of the variability that was in several studies attributed to movement planning may in fact be caused by noise in movement execution.

All the above suggests that, in most common conditions, the effects of localization and planning on movement variability are much smaller than those of movement execution. However, there are many reports of endpoint variability that cannot be explained by noise in movement execution. We will now discuss these studies. Most of these studies employed experimental manipulations that produced a large localization variance. A common manipulation is to turn the targets off and ask subjects to point at their remembered location. This increases the localization variance, as is shown by the rapid increase of variance with memory delay (McIntyre et al. 1997). When the delay is short (0.5 s), the axis of maximum variability has an orientation that could well be expected from a combination of variability due to localization and to execution of about equal magnitude (Carrozzo et al. 1999). For longer delays (several seconds), the localization variance will be much larger than the execution variance, so the latter can be neglected. The shape of the endpoint distribution is therefore almost exclusively determined by how precisely the target location can be memorized, which leads to endpoint distributions whose axis of maximum variability points toward the eyes (McIntyre et al. 1997). This also explains why, in such conditions, the endpoint variability is practically insensitive to manipulations that change the variability due to movement execution, such as changing the movement direction (McIntyre et al. 1997), movement distance (Lemay and Proteau 2001), movement speed (Adamovich et al. 1994), or allowing subjects to see their hand during pointing (Carrozzo et al. 1999; McIntyre et al. 1998). The fact that, in these conditions, the endpoint variability reflects the precision of the memorized target location is very evident when the various targets are placed in an easy to remember geometrical configuration, such as on a straight line. Subjects then build up a representation of the line that allows them to remember the target position relative to the line rather than relative to themselves. The axis of maximum variability therefore tends to align with the target configuration line rather than with the line toward the eyes (Carrozzo et al. 2002; Rossetti 1998).

We conclude that in most common conditions variability in goal-directed arm movements is mainly due to noise in movement execution. This is a combination of noise in the magnitude and noise in the duration of the motor output. As a result, the variability in movement endpoints, and therefore the success rate of reaching the target, depends on the chosen movement trajectory. Given these effects of execution noise on the actual trajectory that we make, we suggest that an important goal of movement control may be to plan movements in such a way that the expected likelihood of missing the target is minimal (Harris and Wolpert 1998).

APPENDIX

Here we present the equations used in the transformation between finger trajectories and motor commands (see also Fig. 2). Indices 1 and 2 refer to the shoulder and elbow joint, respectively.

Kinematics

The finger position (x, y) relative to the shoulder (as defined in Fig. 1*B*) follows from the joint angles (forward kinematics)

$$x = l_1 \cos q_1 + l_2 \cos (q_1 + q_2)$$
$$y = l_1 \sin q_1 + l_2 \sin (q_1 + q_2) \quad \text{(A1)}$$

where l_1 and l_2 denote the lengths of the upper arm (the distance from shoulder to elbow) and forearm (the distance from the elbow to the tip of the index finger), and q_1 and q_2 are the shoulder and elbow angles, respectively, as defined in Fig. 1*B*. The arm lengths were measured for all subjects.

These equations can be inverted to obtain the joint angles expressed as a function of finger position (inverse kinematics)

$$q_2 = \arccos\left(\frac{x^2 + y^2 - l_1^2 - l_2^2}{2 l_1 l_2}\right)$$
$$q_1 = \arctan\left(\frac{y}{x}\right) - \arctan\left(\frac{l_2 \sin q_2}{l_1 + l_2 \cos q_2}\right) \quad \text{(A2)}$$

Dynamics

The torques $\vec{\tau} = (\tau_1, \tau_2)^T$ at the two joints were calculated from the joint angles $\vec{q} = (q_1, q_2)^T$ using the dynamics equations of a two-link manipulator (e.g., Uno et al. 1989)

$$\vec{\tau} = H\ddot{\vec{q}} + \vec{a} \quad \text{(A3)}$$

with

$$H = \begin{pmatrix} I_1 + I_2 + 2m_2 l_1 c_2 \cos q_2 + m_2 l_1^2 & I_2 + m_2 l_1 c_2 \cos q_2 \\ I_2 + m_2 l_1 c_2 \cos q_2 & I_2 \end{pmatrix} \quad \text{(A4)}$$

$$\vec{a} = \begin{pmatrix} -m_2 l_1 c_2 (2\dot{q}_1 + \dot{q}_2)\dot{q}_2 \sin q_2 + b_1 \dot{q}_1 \\ m_2 l_1 c_2 \dot{q}_1^2 \sin q_2 + b_2 \dot{q}_2 \end{pmatrix} \quad \text{(A5)}$$

Here, m_i, c_i, b_i, and I_i represent the mass, the distance of the arm segment's center of mass from the joint, the viscosity coefficient, and moment of inertia of arm segment i (=1, 2) around the joint, respectively. The values for the mass, moment of inertia, and center of mass of each arm segment were taken from Kawato (1995) and scaled according to the actual lengths. The viscosity coefficient of both joints was set to 0.8 kg m^2/s (Nakano et al. 1999).

These equations were used to calculate the joint torques from the observed joint angles (inverse dynamics). To calculate joint angles from torques (forward dynamics), we inverted *Eq. A3*

$$\ddot{\vec{q}} = H^{-1}(\vec{\tau} - \vec{a}) \quad \text{(A6)}$$

and integrated this numerically to determine the joint angles from the torque profiles.

Muscle model

We used a muscle model to estimate the motor commands u from the joint torques. The shoulder and elbow muscles were modeled as two second-order linear muscles with time constants t_e and t_a of 30 and 40 ms, representing excitation and activation (van der Helm and Rozendaal 2000)

$$u_i = t_e t_a \dddot{\tau}_i + (t_e + t_a)\ddot{\tau}_i + \dot{\tau}_i + \tau_i \quad \text{(A7)}$$

ACKNOWLEDGMENTS

We thank P. Baraduc for helping to run *experiment 3*.

GRANTS

This work was supported by Biotechnology and Biological Sciences Research Council Grant 31/SO 9539, Netherlands Organization for Scientific Research (NWO) Grant 451-02-013, the Wellcome Trust, the Human Frontiers Science Program, and the McDonnell Foundation.

REFERENCES

Adamovich S, Berkinblit M, Smetanin B, Fookson O, and Poizner H. Influence of movement speed on accuracy of pointing to memorized targets in 3D space. *Neurosci Lett* 172: 171–174, 1994.

Akaike H. Information theory as an extension of the maximum likelihood principle. In: *Second International Symposium on Information Theory*, edited by Petrov BN and Csaki F. Budapest: Akademiai Kiado, 1973, p. 267–281.

Atkeson CG and Hollerbach JM. Kinematic features of unrestrained vertical arm movements. *J Neurosci* 5: 2318–2330, 1985.

Buneo CA, Boline J, Soechting JF, and Poppele RE. On the form of the internal model for reaching. *Exp Brain Res* 104: 467–479, 1995.

Carrozzo M, McIntyre J, Zago M, and Lacquaniti F. Viewer-centered and body-centered frames of reference in direct visuomotor transformations. *Exp Brain Res* 129: 201–210, 1999.

Carrozzo M, Stratta F, McIntyre J, and Lacquaniti F. Cognitive allocentric representations of visual space shape pointing errors. *Exp Brain Res* 147: 426–436, 2002.

Chernikoff T and Taylor F. Reaction time to kinaesthetic stimulation resulting from sudden arm displacement. *J Exp Psychol* 43: 1–8, 1952.

Conti P and Beaubaton D. Role of structured visual field and visual reafference in accuracy of pointing movements. *Percept Mot Skills* 50: 239–244, 1980.

Cordo P, Carlton L, Bevan L, Carlton M, and Kerr GK. Proprioceptive coordination of movement sequences: role of velocity and position information. *J Neurophysiol* 71: 1848–1861, 1994.

Cordo PJ. Kinesthetic control of a multijoint movement sequence. *J Neurophysiol* 63: 161–172, 1990.

Desmurget M, Jordan M, Prablanc C, and Jeannerod M. Constrained and unconstrained movements involve different control strategies. *J Neurophysiol* 77: 1644–1650, 1997.

Desmurget M, Rossetti Y, Prablanc C, Stelmach GE, and Jeannerod M. Representation of hand position prior to movement and motor variability. *Can J Physiol Pharmacol* 73: 262–272, 1995.

Eliason SR. *Maximum Likelihood Estimation: Logic and Practice.* Thousand Oaks, CA: Sage Publications, 1993.

Fisher NI. *Statistical Analysis of Circular Data.* Cambridge, UK: Cambridge, 1993.

Fitts PM. The information capacity of the human motor system in controlling the amplitude of movement. *J Exp Psychol* 47: 381–391, 1954.

Ghez C, Gordon J, Ghilardi MF, Christakos CN, and Cooper SE. Roles of proprioceptive input in the programming of arm trajectories. *Cold Spring Harb Symp Quant Biol* 55: 837–847, 1990.

Gordon J, Ghilardi MF, Cooper SE, and Ghez C. Accuracy of planar reaching movements. II. Systematic extent errors resulting from inertial anisotropy. *Exp Brain Res* 99: 112–130, 1994a.

Gordon J, Ghilardi MF, and Ghez C. Accuracy of planar reaching movements. I. Independence of direction and extent variability. *Exp Brain Res* 99: 97–111, 1994b.

Gribble PL, Mullin LI, Cothros N, and Mattar A. Role of cocontraction in arm movement accuracy. *J Neurophysiol* 89: 2396–2405, 2003.

Haggard P and Richardson J. Spatial patterns in the control of human arm movement. *J Exp Psychol Hum Percept Perform* 22: 42–62, 1996.

Hansen RM and Skavenski AA. Accuracy of eye position information for motor control. *Vision Res* 17: 919–926, 1977.

Harris CM and Wolpert DM. Signal-dependent noise determines motor planning. *Nature* 394: 780–784, 1998.

Hogan N. The mechanics of multi-joint posture and movement control. *Biol Cybern* 52: 315–331, 1985.

Hollerbach JM and Flash T. Dynamic interactions between limb segments during planar arm movement. *Biol Cybern* 44: 67–77, 1982.

Ivry RB and Hazeltine RE. Perception and production of temporal intervals across a range of durations: evidence for a common timing mechanism. *J Exp Psychol Hum Percept Perform* 21: 3–18, 1995.

Jaric S, Tortoza C, Fatarelli IFC, and Almeida GL. Effects of direction and curvature on variable error pattern of reaching movements. *Motor Control* 3: 414–423, 1999.

Jones KE, Hamilton AF de C, and Wolpert DM. Sources of signal-dependent noise during isometric force production. *J Neurophysiol* 88: 1533–1544, 2002.

Kawato M. Unidirectional versus bi-directional theory for trajectory planning and control. In: *Mathematical Approaches to Fluctuations: Complexity and Nonlinearity 2,* edited by Hida T. Singapore: World Scientific Ltd., 1995, p. 144–180.

Koshland GF, Marasli B, and Arabyan A. Directional effects of changes in muscle torques on initial path during simulated reaching movements. *Exp Brain Res* 128: 353–368, 1999.

Lemay M and Proteau L. A distance effect in a manual aiming task to remembered targets: a test of three hypotheses. *Exp Brain Res* 140: 357–368, 2001.

McIntyre J, Stratta F, and Lacquaniti F. Viewer-centered frame of reference for pointing to memorized targets in three-dimensional space. *J Neurophysiol* 78: 1601–1618, 1997.

McIntyre J, Stratta F, and Lacquaniti F. Short-term memory for reaching to visual targets: psychophysical evidence for body-centered reference frames. *J Neurosci* 18: 8423–8435, 1998.

Messier J and Kalaska JF. Differential effect of task conditions on errors of direction and extent of reaching movements. *Exp Brain Res* 115: 469–478, 1997.

Messier J and Kalaska JF. Comparison of variability of initial kinematics and endpoints of reaching movements. *Exp Brain Res* 125: 139–152, 1999.

Meyer DE, Abrams RA, Kornblum S, Wright CE, and Smith JEK. Optimality in human motor performance: ideal control of rapid aimed movements. *Psychol Rev* 95: 340–370, 1988.

Miall RC and Wolpert DM. Forward models for physiological motor control. *Neural Network* 9: 1265–1279, 1996.

Moore BR. A modification of the Rayleigh test for vector data. *Biometrika* 67: 175–180, 1980.

Nakano E, Imamizu H, Osu R, Uno Y, Gomi H, Yoshioka T, and Kawato M. Quantitative examinations of internal representations for arm trajectory planning: minimum commanded torque change model. *J Neurophysiol* 81: 2140–2155, 1999.

Newell KM and Houk JC. Speed and accuracy of compensatory responses to limb disturbances. *J Exp Psychol Hum Percept Perform* 9: 58–74, 1983.

Pastor AM, Torres B, Delgado-Garcia JM, and Baker R. Discharge characteristics of medial rectus and abducens motoneurons in the goldfish. *J Neurophysiol* 66: 2125–2140, 1991.

Rossetti Y. Implicit short-lived motor representations of space in brain damaged and healthy subjects. *Conscious Cogn* 7: 520–558, 1998.

Rossetti Y, Stelmach G, Desmurget M, Prablanc C, and Jeannerod M. The effect of viewing the hand prior to movement onset on pointing kinematics and variability. *Exp Brain Res* 101: 323–330, 1994.

Schmidt RA, Zelaznik H, Hawkins B, Frank JS, and Quinn JT. Motor-output variability: a theory for the accuracy of rapid motor acts. *Psychol Rev* 86: 415–451, 1979.

Slifkin AB and Newell KM. Noise, information transmission, and force variability. *J Exp Psychol Hum Percept Perform* 25: 837–851, 1999.

Suzuki M, Shiller DM, Gribble PL, and Ostry DJ. Relationship between cocontraction, movement kinematics and phasic activity in single-joint movement. *Exp Brain Res* 140: 171–181, 2001.

Todorov E and Jordan MI. Optimal feedback control as a theory for motor coordination. *Nature Neurosci* 5: 1226–1235, 2002.

Uno Y, Kawato M, and Suzuki R. Formation and control of optimal trajectory in human multijoint arm movement. Minimum torque-change model. *Biol Cybern* 61: 89–101, 1989.

van Beers RJ, Sittig AC, and Denier van der Gon JJ. How humans combine simultaneous proprioceptive and visual position information. *Exp Brain Res* 111: 253–261, 1996.

van Beers RJ, Sittig AC, and Denier van der Gon JJ. The precision of proprioceptive position sense. *Exp Brain Res* 122: 367–377, 1998.

van Beers RJ, Sittig AC, and Denier van der Gon JJ. Integration of proprioceptive and visual position-information: an experimentally supported model. *J Neurophysiol* 81: 1355–1364, 1999.

van den Dobbelsteen JJ, Brenner E, and Smeets JBJ. Endpoints of arm movements to visual targets. *Exp Brain Res* 138: 279–287, 2001.

van der Helm FCT and Rozendaal LA. Musculoskeletal systems with intrinsic and proprioceptive feedback. In: *Biomechanics and Neural Control of Posture and Movement*, edited by Winters JM and Crago PE. New York: Springer, 2000, p. 164–174.

van Galen GP and de Jong WP. Fitts' law as the outcome of a dynamic noise filtering model of motor control. *Hum Mov Sci* 14: 539–571, 1995.

Vince MA. Corrective movements in a pursuit task. *Q J Exp Psychol* 1: 85–106, 1948.

Vindras P and Viviani P. Frames of reference and control parameters in visuomanual pointing. *J Exp Psychol Hum Percept Perform* 24: 569–591, 1998.

Wing AM and Kristofferson AB. Response delays and the timing of discrete motor responses. *Percept Psychophys* 14: 5–12, 1973.

Wolpert DM, Ghahramani Z, and Jordan MI. An internal model for sensorimotor integration. *Science* 269: 1880–1882, 1995.

Woodworth RS. The accuracy of voluntary movement. *Psychological Review Monograph*, 3: 1–114, 1899.

Zar JH. *Biostatistical Analysis* (4th ed.). Upper Saddle River, NJ: Prentice-Hall, 1999.